Evaluation of the cross reactivity of neutralising antibody response in vaccinated human and convalescent hamster sera against SARS-CoV-2 variants up to and including JN.1 using an authentic virus neutralisation assay

Naomi S. Coombes[1*], Kevin R. Bewley[1], Yann Le Duff[2], Nassim Alami-Rahmouni[2], Kathryn A. Ryan[1], Sarah Kempster[2], Deborah Ferguson[2], Elizabeth R. Davies[1], Thomas M. Weldon[1], Eleanor S. Cross[1], Lauren Smith[1], Conner Norris[1], Karly Rai Rogers-Broadway[1], Kuiama Lewandowski[1], Samantha Treagus[1], Isobel Everall[1], Steven T. Pullan[1], Bassam Hallis[1], Sue Charlton[1], Yper Hall[1], Simon G. P. Funnell[1,3,4]

1 UK Health Security Agency, Porton Down, Salisbury, Wiltshire, United Kingdom

2 Scientific Research and Innovation, Medicines and Healthcare products Regulatory Agency, South Mimms, United Kingdom.

3 Quadram Institute Bioscience, Rosalind Franklin Road, Norwich Research Park, Norfolk, UK

4 World Health Organisation, Geneva, Switzerland

* Corresponding author

E-mail: naomi.coombes@ukhsa.gov.uk (NC)

23

24 **Abstract**

25 New vaccines, therapeutics and immunity elicited by natural infection create evolutionary pressure
26 on SARS-CoV-2 to evolve and adapt to evade vaccine-induced and infection-elicited immunity.
27 Vaccine and therapeutics developers thus find themselves in an "arms race" with the virus. The
28 ongoing assessment of emerging SARS-CoV-2 variants remains essential as the global community
29 transitions from an emergency response to a long-term management plan. Here, we describe how
30 an authentic virus neutralisation assay using low passage clinical virus isolates has been employed to
31 monitor resistance of emerging virus variants to neutralising antibodies from humans and
32 experimentally infected hamsters. Sera and plasma from people who received three doses of a
33 vaccine as well as those who received a bivalent booster were assessed against SARS-CoV-2 variants,
34 up to and including JN.1. Contemporary or recent virus variants showed substantial resistance to
35 neutralisation by antibodies from those who had received three doses of an ancestral vaccine but
36 were still effectively neutralised by antibodies from individuals who had received a bivalent booster
37 (ancestral/BA.1). In our recent studies, however, the JN.1 VOI was found to be significantly more
38 resistant to neutralisation by antibodies from those who had received the ancestral/BA.1 bivalent
39 boost. Convalescent sera from hamsters that had been experimentally infected with one of seven
40 virus variants (ancestral, BA.1, BA.4, BA.5.2.1, XBB.1.5, XBB.1.16, XBB.2.3) were also tested here. The
41 recent contemporary variant, BA.2.86, was effectively neutralised by sera from hamsters infected
42 with XBB.1.5 and XBB.1.16 but it was not neutralised by sera from those infected with BA.5.2.1.
43 These data support the recommendations given by the WHO that a new vaccine was required and
44 should consist of an XBB sub-lineage antigen.

45 **Introduction**

46 Coronavirus 2019 disease (COVID-19) caused by SARS-CoV-2 continues to cause significant
47 disruption to healthcare systems and economies worldwide having caused over 774 million cases

48 and 7.01 million deaths since its emergence in December 2019 (as of January 2024) [1]. The WHO
49 downgraded the COVID-19 pandemic from a public health emergency of international concern
50 (PHEIC) on 5 May 2023, this marked a transition from emergency response to long-term
51 management [2]. However, the virus continues to evolve in response to changing population
52 immunity leading to the regular identification of new viral variants. Sequences of emerging variants
53 are continuously monitored and assigned as new sub-lineages by the Phylogenetic Assignment of
54 Named Global Outbreak Lineages (PANGOLIN) tool. At the time of writing there are 3,569 designated
55 SARS-CoV-2 lineages with five of these having been classified as variants of concern (VOC) by the
56 WHO Technical Advisory Group on Virus Evolution: Alpha (B.1.1.7), Beta (B.1.351), Delta (B.1.617.2),
57 Gamma (P.1) and Omicron (B.1.1.529) [3-5].

58 A global effort to design and manufacture COVID-19 vaccines began as soon as the viral genome was
59 published and the first COVID-19 vaccine was deployed in the UK on 8th December 2020 (Comirnaty)
60 [6]. This was followed by Vaxzevria on 30th December 2020 and Spikevax on 8th January 2021 [7, 8].
61 These vaccines were the most widely used worldwide for the initial course of three immunisations
62 and all were based on the ancestral (clade A) virus spike glycoprotein. In the first year of vaccines
63 being available it has been predicted that vaccination prevented as many as 14.4 million deaths due
64 to COVID-19 [9]. The emergence of novel SARS-CoV-2 variants brought with it the concern that
65 ancestral-based vaccines would no longer provide sufficient protection to vulnerable people in at-
66 risk groups. Indeed, our data utilising the gold-standard authentic virus neutralisation assay
67 indicated that the latest variants were becoming increasingly resistant to ancestral-based immune
68 responses [10-12]. Bivalent vaccines were developed in response to this concern and have been
69 designed to not only target the ancestral strain but also Omicron sub-lineage spike glycoproteins.
70 These were approved for use in the UK (BA.1/ancestral bivalent) for at-risk groups only in the
71 Autumn of 2022, and the US (BA.5/ancestral bivalent) for anyone aged 18 or over in August 2022
72 [13, 14]. Restricting vaccination to only at-risk groups in the UK and low vaccine uptake in the US,
73 where only 34% adults received a fourth booster, means that most of the population who have

74 received a vaccination are still immunised with an ancestral spike-based vaccine [15]. However, since
75 the relaxing of restrictions worldwide, many people will also have received some degree of natural
76 immunity due to infection with one or more of the circulating variants. The most recent vaccines to
77 be approved elicit immunity against contemporary XBB recombinants, the latest to gain
78 authorisation consists of an XBB.1.5 component [16-18].

79 The recent emergence of the BA.2.86 variant and its subvariants such as JN.1 has highlighted the
80 value of sustained sequence monitoring due to the sudden appearance of a virus with vastly
81 different spike sequence compared to other circulating variants or those represented in the latest
82 vaccines. As part of a CEPI-funded "Agility" project, we have been monitoring and performing risk
83 assessments of SARS-CoV-2 variants since November 2020. We previously presented our analysis of
84 20 different variants using early pandemic human convalescent and triple-vaccinated plasma and
85 serum panels as well as international standards [12]. Here we describe our latest data generated
86 using serum or plasma collected from a panel of individuals who have received up to four doses of a
87 COVID-19 vaccine using an authentic virus neutralisation assay. These assays have been performed
88 using well characterised, low passage SARS-CoV-2 viruses derived from clinical isolates including the
89 BA.2.86 and JN.1 variants. We also present neutralisation data generated using the sera of
90 experimentally infected hamsters which were convalescent from either the ancestral virus (pre-
91 D614G), BA.1, BA.4, BA.5.2.1, XBB.1.5, XBB.1.16 or XBB.2.3 (mono-variant convalescent). We have
92 also compared the antigenic maps of these two data sets.

93 **Results**

94 Through monitoring of the currently circulating SARS-CoV-2 variants, we identified and sourced
95 nasopharyngeal swabs from sequence-confirmed patients through our clinical networks and Pillar 1
96 testing (primarily positive tests conducted in primary healthcare settings) in England. We then used
97 an authentic virus FRNT using low passage SARS-CoV-2 variants of clinical origin to perform risk
98 assessments with regards to cross-reactivity of humoral immunity. SISPA-Illumina sequencing was

99 performed on stocks prior to use in the FRNT to confirm the lineage and check for cell culture-
100 induced mutations. We note that one of the BA.2.86 variants (BA.2.86 – A) described here contains
101 an unexpected amino acid change within the furin cleavage site (FCS) (S:R682W). However, work
102 published by others indicates that changes in this position are unlikely to alter the neutralisation
103 profile, though this mutation makes this stock unsuitable for *in vivo* studies [19-22]. Neutralisation
104 assays were therefore performed with this virus whilst efforts continued to generate a bank of
105 BA.2.86 with a wild-type FCS (BA.2.86 – B). The variants used in this study, and their sources, are
106 detailed in Table 1.

107

Table 1 – SARS-CoV-2 variants used in this study

WHO Designation	Pangolin Lineage	GISAID Clade/Lineage	Nextstrain Clade	Date Assigned	GISAID ID of Isolation Swab (Where Known) and/or Source
Ancestral virus	B	O	19A	Jan 2020	EPI_ISL_406844
Alpha	B.1.1.7	GRY	20I (V1)	Dec 2020	EPI_ISL_683466
Beta	B.1.351	GH/501Y.V2	20H (V2)	Dec 2020	EPI_ISL_770441
Delta	B.1.617.2	G/452R.V3	21A	May 2021	EPI_ISL_2742236
Zeta–FioCruz *	P.2	GR/484K.V2	20B/S.484K	Mar 2021	FioCruz, Brazil
Zeta–BEI *	P.2	GR/484K.V2	20B/S.484K	Mar 2021	BEI (NR-55439)
XE	XE	GRA	Recombinant	Mar 2022	EPI_ISL_11586931
XF	XF	GRA	Recombinant	Mar 2022	EPI_ISL_10458256
Omicron	BA.1	GRA	21K	Dec 2021	EPI_ISL_7400555
Omicron	BA.1.1	GRA	21K	Jan 2022	EPI_ISL_8165999
Omicron	BA.2	GRA	21L	Dec 2021	Not available
Omicron	BA.2.12.1	GRA	22C	Apr 2022	Gavin Screaton (University of Oxford)
Omicron	BA.2.75.3	GRA	22D	Jun 2022	EPI_ISL_13882158
Omicron	BA.2.75.2	GRA	22D	Aug 2022	Not available
Omicron	BA.4	GRA	22A	Apr 2022	EPI_ISL_13157810
Omicron	BA.4.6	GRA	22A	Jul 2022	Not available
Omicron	BA.5.2.1	GRA	22B	Apr 2022	EPI_ISL_12810908
Omicron	BQ.1.22	GRA	22E	Sep 2022	EPI_ISL_15581064
XBB.1.1	XBB.1.1	GRA	22F	Oct 2022	EPI_ISL_15682231
Omicron	CH.1.1	GRA	23C	Oct 2022	EPI-ISL-16615644
XBB.1.5	XBB.1.5	GRA	23A	Jan 2023	EPI-ISL-16587654
XBB.1.16	XBB.1.16	GRA	23B	Mar 2023	EPI_ISL_17666853
XBB.2.3	XBB.2.3	GRA	23E	Jan 2023	Not available
EG.5.1.1	EG.5.1.1	GRA	23F	Jun 2023	EPI_ISL_18355898
Omicron*	BA.2.86 (A)	GRA	21L	Aug 2023	EPI_ISL_18111770
Omicron*	BA.2.86 (B)	GRA	21L	Aug 2023	EPI_ISL_18274087
Omicron	JN.1	GRA	21L	Sep 2023	EPI_ISL_18521510

* For Zeta and BA.2.86, assays were conducted with stocks derived from viruses of different sources.

108

109 Our previously published data indicated that immunity derived from neutralising antibodies was
110 becoming less effective for those who had received three doses of a first-generation COVID-19
111 vaccine against the currently circulating variants [12]. Whilst a newer panel of sera was acquired, we
112 continued our assessment of triple vaccinated individuals who had received an original ancestral
113 based vaccine. This panel had been tested against ten SARS-CoV-2 variants (including ancestral) at
114 the point of publishing our previous paper. We have subsequently tested this panel against a further
115 six variants (Zeta – FC, Zeta – BEI, BA.4.6, BA.2.75.2, BQ.1.22 and XBB.1.1), as shown in Figure 1.

116 Our previous report demonstrated a significant difference in ND_{50} titres of our pre-Alpha
117 convalescent panel when tested against two different Zeta isolates. This was notable due to most
118 other published data for this variant demonstrating comparable neutralisation titres to those against
119 Delta. However, another group demonstrated a similarly large resistance to neutralisation of Zeta
120 with a panel of early convalescent sera but not a panel of vaccinee sera [23]. We therefore sought to
121 investigate whether the same pattern would be observed with our triple vaccinee panel (Figure 1).
122 Geometric mean ND_{50} neutralisation titres (GM) of this panel against Zeta – FC and Zeta – BEI were
123 199 and 671 corresponding to a 26.2-fold and 7.8-fold reduction relative to ancestral, respectively.
124 The difference between the titres measured against the two Zetas was significant (fold-change = 3.4;
125 ME-ANOVA; $p < 0.05$). Of the four remaining additional variants that were tested against this panel
126 since our previous paper, BA.4.6 and BA.2.75.2 resulted in GM titres above the lower limit of
127 detection of the assay (LLOD), thus permitting more accurate estimates of fold-reduction relative to
128 ancestral virus. The fold-reduction for BA.4.6 relative to ancestral was statistically significant at 105.
129 When compared to its close parent lineage, BA.4, there was also a significant fold-reduction of 2.1.
130 Against BA.2.75.2 the triple-vaccinated panel gave a GM titre of 46.1 which equated to a 113-fold
131 reduction relative to ancestral and 3.7-fold reduction relative to a closely related variant, BA.2.75.3.
132 Two of the most recent variants (BQ.1.22 and XBB.1.1) were substantially resistant to neutralisation
133 to sera from triple-vaccinated individuals with most titres falling below the LLOD. Sera which fall
134 below the LLOD are assigned the value of the lowest dilution used in the assay (1/20), thus fold-

135 reduction calculations do not provide accurate estimates. The lower limit of quantification (LLOQ)
136 for the ancestral virus assay (previously determined as 58) is also displayed [11]. Although the LLOQ
137 was not determined for subsequent variants, the precision of the assay is likely to be lower for titres
138 falling below this value. However, the estimated fold-reductions relative to ancestral virus for
139 BQ.1.22 and XBB.1.1 were estimated at 197 and 226-fold.

140 In addition, to assessing the sera from individuals of the panel, the neutralisation titres of the NIBSC
141 working reagents 21/234 and/or International Standard 21/338 were also assessed in every assay.
142 These are displayed in Figure 1 as green squares or blue circles, respectively. As described
143 previously, these are pools of pre-Alpha convalescent plasma (21/234) or individuals who were both
144 vaccinated and convalescent following an Alpha, Beta or Delta infection (21/338). These standards
145 are typically more potent at neutralising the virus compared to the panel. However, it was noted
146 that for BA.2.75.2, BA.4, BA.4.6 and BA.5.2.1, the 21/234 standard was yielding ND_{50} values
147 comparable to those from the lowest responders of our panel and was completely unable to
148 neutralise BQ.1.22. The newest 21/338 standard retains good reactivity and ability to neutralise all
149 variants assessed herein.

150 To continue to assess humoral immunity to currently circulating SARS-CoV-2 variants, a selection of
151 participants who had received a fourth (booster) vaccine were sought. A panel of 22 individuals was
152 assembled from donations given by eight MHRA staff members and 14 UKHSA staff members who
153 had received three doses of a first-generation COVID-19 vaccine followed by a booster with a
154 bivalent (BA.1/ancestral) vaccine. Samples were collected a median of 78 days after the most recent
155 vaccination. Among the 22 individuals, 19 had a known previous SARS-CoV-2 infection between
156 February 2021 and December 2022.

157 This four-dose panel was first assessed against the ancestral virus which resulted in the highest
158 neutralisation titres with a GM of 12,400 (Figure 2). Next, we assessed the titres of this panel against
159 one of the earlier Omicron sub lineages, BA.4. The GM neutralisation titres of the panel against BA.4

160 was 624.0 which equated to a 19.8-fold reduction relative to ancestral virus. To date this panel has
161 been tested against a further nine variants. One of these variants with a large resistance to
162 neutralising antibodies was CH.1.1 with a GM titre for the panel of 68.7 and fold-reduction of 180.
163 Another Omicron sub lineage, BQ.1.22, also displayed notable resistance to neutralisation by the
164 four-dose panel which generated a GM titre of 102.0 corresponding to a 121.9-fold-reduction
165 relative to ancestral virus. The recombinants, XBB.1.1, XBB.1.5, XBB.1.16, XBB.2.3 and EG.5.1.1 all
166 gave comparable GM titres between 82.9 and 137.0. Similarly, the recently emerged Omicron sub-
167 lineage, BA.2.86, was neutralised equally well by those who have had received four doses of a
168 COVID-19 vaccine. Here, we tested two BA.2.86 isolates with or without an FCS substitution
169 (S:R682W), BA.2.86 – A and BA.2.86 – B, respectively. The GM titres of the panel against each virus
170 was 99.3 and 97.0, equating to a 124.7 and 127.6-fold reduction relative to ancestral, respectively.
171 There was no significant difference between BA.2.86 – A and BA.2.86 – B ($p=1.00$). The variant
172 tested here with the largest resistance to neutralisation was the Omicron sub lineage, JN.1. The GM
173 titre for the panel against JN.1 was observed to be 28.9 which represents a 428.9-fold reduction
174 relative to the ancestral virus and 3.4 lower fold-reduction relative to BA.2.86 (A and B, $p<0.05$).

175 The international standard 21/338 was able to effectively neutralise all previous variants but only
176 yielded a neutralisation titre of 22 against JN.1, which is nearing the LLOD (20). In addition, 12 of the
177 22 four-dose panel samples gave titres at or below the LLOD when tested against JN.1. The
178 numerical breakdown of these data and the model estimates of geometric means are presented in
179 Table S2.

180 Antigenic cartography is a powerful method for visualising the evolution of a pathogen by plotting
181 the neutralisation titres of different panels of sera against successive variants or strains. It was
182 originally developed as a means of monitoring changes in seasonal influenza virus and has since
183 been used by numerous groups to compare SARS-CoV-2 variants [24-26]. Here, we use this
184 technique to visualise the antigenic relationships of the SARS-CoV-2 variants tested against the

185 panels of human sera or plasma described in this and our previous publication (Figure 3). The data
186 plotted here include all titres from a panel of pre-Alpha convalescent plasma, triple-vaccinated
187 individuals, boosted (BA.1/ancestral bivalent) individuals and the three standards (20/136, 21/334,
188 21/338). Each square of the map represents one antigenic unit which equates to a two-fold change
189 in neutralisation titres. The ancestral virus is presented as a red circle and sits in the centre of the
190 serum panels. Pre-Omicron variants were coloured as dark green circles and are situated within an
191 inner circle around the serum panels. In the influenza field, vaccines are updated when circulating
192 strains are at least two units away from the vaccine strain, thus marking it as genetically different
193 [25]. Of the pre-Omicron variants, Beta and Zeta-FC are the furthest from ancestral virus with a gap
194 of over 4 antigenic units, though in perpendicular directions from ancestral. Substantial diversity can
195 be seen in post-Omicron variants which are grouped and coloured as Omicron-BA.1x (light green),
196 Omicron-BA.2.x (sky blue), Omicron-BA.4/5.x (yellow), late Omicron (lilac), XE/XF recombinants
197 (pink) and XBB recombinants (neon blue). However, some patterns can be seen, for example the
198 recombinants XF and XE cluster with the virus from which their spike was derived. The recombinant
199 XF is located with BA.1/BA.1.1 at approximately 5.5 units from ancestral and XE with BA.2/BA.2.12.1
200 at 4.5 units from ancestral. Also, the BA.4 and BA.5.2.1 cluster closely at approximately 5.5 units
201 away from ancestral and, while the BA.4.6 sub lineage is a similar distance from ancestral, it is also
202 approximately 4.5 units away from its parent, BA.4. The XBB family of variants cluster together at
203 approximately 5.5 units from ancestral and within this cluster there are 1.2 antigenic units between
204 the two most distant variants, XBB.1.16 and EG.5.1.1. The late Omicron variants (BQ.1.22, CH.1.1
205 and BA.2.86) form another separate cluster approximately seven antigenic units from ancestral with
206 JN.1 approximately one antigenic unit further away from this cluster. Interestingly, BA.2.75.2 and
207 BA.2.75.3 appear on the opposite side of the map to BA.2 with BA.2.75.2 located closer to the late
208 Omicrons than to BA.2.75.3.

209 One of the known limitations of generating antigenic maps with human neutralisation data is the
210 diversity of pre-existing immunity that is associated with multi-exposure sera (vaccine and naturally

211 acquired). We therefore used single-exposure convalescent sera collected during our *in vivo* hamster
212 infection studies to generate more antigenically defined maps. In Figure 4, we have plotted
213 neutralisation titres of sera from hamsters collected on day 27 (ancestral and BA.1) or day 28 (BA.4,
214 BA.5.2.1, XBB.1.5, XBB.1.16, XBB.2.3) after a single virus infection by the intranasal route. Each panel
215 of sera was tested against the variant used as the challenge virus. Fold-changes against subsequent
216 variants tested are presented as relative to the virus used for infection (Figure 4). Data for hamsters
217 infected with ancestral, BA.1, BA.4 and BA.5.2.1 are described previously but also presented here
218 [27, 28]. As our results from the human data indicated that the FCS substitution in the BA.2.86 – A
219 virus did not affect neutralisation titres, repeat assays with these volume-limited sera were not
220 performed with the second virus.

221 Briefly, sera taken from hamsters infected with ancestral virus gave significantly lower GM titres
222 with a 3.3- and 3.5-fold reduction for Alpha and Delta relative to ancestral, respectively. Sera taken
223 from BA.1 convalescent hamsters showed a similar ability to neutralise both BA.1 and ancestral but
224 were unable to neutralise BQ.1.22 and XBB.1.1 at the lowest dilution used here (1/30). For BA.4
225 convalescent hamster sera, BQ.1.22 and XBB.1.5 were the only variants which were significantly
226 more resistant to neutralisation by these sera, with the latter resulting in GM titres all below the
227 LLOD. In hamsters that were convalescent for BA.5.2.1, GM titres against ancestral virus relative to
228 BA.5.2.1 were not significantly different. Titres against all other variants tested against BA.5.2.1
229 convalescent sera were significantly lower relative to BA.5.2.1. Against BQ.1.22, XBB.1.1, XBB.1.5
230 and EG.5.1.1 titres were above the LLOD meaning fold changes could be determined accurately with
231 7.5-, 94.4-, 80.1-, 73.8-fold reductions, respectively. Notably, when tested against BA.2.86 – A, none
232 of the sera from BA.5.2.1 infected hamsters were able to neutralise the virus with all titres falling
233 below the LLOD. GM titres of convalescent sera from hamsters infected with XBB.1.5 tested against
234 EG.5.1.1 were significantly reduced relative to XBB.1.5 with a 1.8-fold reduction. When these sera
235 were tested against BA.2.86 there was no significant difference in GM neutralising titres.
236 Convalescent sera from hamsters experimentally infected with XBB.1.16 were tested against

237 ancestral virus, Beta, BA.1, BA.5.2.1, XBB.1.5, EG.5.1.1, XBB.2.3 and BA.2.86 – A. GM titres for this
238 panel against all variants were significantly reduced relative to XBB.1.16 with fold-reductions of 6.0,
239 77.5, 55.0, 17.1, 6.8, 10.4, 12.2 and 33.1, respectively. Finally, convalescent sera from hamsters
240 experimentally infected with XBB.2.3 were able to neutralise ancestral, XBB.1.16 and EG.5.1.1
241 equally well to XBB.2.3. Against all other variants (Beta, BA.1, BA.5.2.1, XBB.1.5, BA.2.86 – A), the
242 neutralisation titres for these sera were significantly lower with Beta displaying the most resistance
243 to neutralisation by this panel. The numerical breakdown of these data and the model estimates of
244 geometric means are presented in Tables S3-S9.

245 When these data were used to generate an antigenic map (Figure 5) the points corresponding to
246 individual sera were more widely distributed compared to the human map. As expected, each
247 antigenic variant clusters with sera from animals infected with homologous virus. Of the pre-
248 Omicron variants, Beta is again the most antigenically distant at approximately three units from
249 ancestral. BQ.1.22 is located in the same area of the map as Beta but another antigenic unit further
250 from ancestral. The most antigenically distinct variant with the hamster map was XBB.1.1 at 5.5 units
251 from ancestral and three units away from the nearest variant on the map, BA.1. The most
252 contemporary variant tested here, BA.2.86 – A, is approximately five units from ancestral but
253 clusters closely to XBB.1.5 with just over one antigenic units' distance.

254 **Discussion**

255 SARS-CoV-2 continues to cause worldwide disruption, despite the downgrading of the COVID-19
256 pandemic marking the end of the public health emergency. Since its emergence, SARS-CoV-2 has
257 been acquiring fitness-enhancing mutations in response to changing population immunity driven by
258 both infection and vaccination [29]. It is thought that additional pressures on the virus such as the
259 clinical use of antiviral drugs, long-term infections in immunocompromised individuals and spillback
260 events from zoonotic infections are also likely to contribute to the increased diversity in viral
261 sequences [30, 31]. Here, we present our updated assessment of emerging SARS-CoV-2 variants in

262 an authentic virus neutralisation assay against panels of sera or plasma from individuals who have
263 received three doses of a COVID-19 vaccine as well as those who received a bivalent (BA.1/ancestral)
264 booster. We also assessed neutralisation titres from experimentally infected hamsters that were
265 convalescent for seven SARS-CoV-2 variants (ancestral, BA.1, BA.4, BA.5.2.1, XBB.1.5, XBB.1.16,
266 XBB.2.3) and map both these and the human data antigenically.

267 In our previous publication we described a distinct difference in neutralisation titres against two
268 different isolates of the Zeta variant when tested against our pre-Alpha convalescent panel. Another
269 group from the University of Geneva showed a similar large reduction in neutralisation titres with an
270 early pandemic convalescent panel of sera against Zeta that was not seen against triple vaccinated
271 individuals [32]. We therefore tested our two Zeta isolates against our three-dose vaccinee panel,
272 however these viruses continued to show substantial resistance to neutralisation by this panel with a
273 significant difference between the two isolates. A sequence comparison with data kindly supplied by
274 the University of Geneva revealed identical spike sequences for all three viruses but with a three
275 amino acid deletion in the N gene of the virus discussed in the Bekliz paper (208-210). Zeta – BEI and
276 the University of Geneva virus also have three additional non-synonymous mutations in Orf1a
277 leading to amino acid changes: V1071A, P1810L and S3149F. With no differences in the main viral
278 proteins exposed to neutralising antibodies (spike, membrane, envelope), it appears that the
279 sequence is not responsible for the variation in titres seen here. Other potential explanations were
280 described in our previous paper and include the potential impact of secretion of free spike protein,
281 defective interfering particles and differences in spike glycosylation [12, 33-37].

282 Our data from individuals who had received three doses of an ancestral spike-based vaccine
283 indicated that antibodies against the two variants, BA.2.75.2 and BA.4.6, were less able to neutralise
284 these viruses with titres nearing the LLOD. BA.2.75.2 has three additional amino acid changes
285 relative to BA.2.75.3 (identical spike to BA.2.75) which are thought to increase immune evasion
286 (S:R346T, S:F486S, S:D1199N) [38, 39]. Similarly, BA.4.6 also contains S:R346T relative to its parent,

287 BA.4. Our neutralisation data supports this prediction with a higher immune escape of BA.2.75.2
288 compared to BA.4.6 and agrees with others who show similar trends [40, 41].

289 Further testing of this population demonstrated that the sera in this panel had no detectable
290 neutralising activity against the later variants, BQ.1.22 and XBB.1.1. The BQ.1.22 variant used in this
291 study has the same spike sequence as the BQ.1.1 variant, which was dominant in December 2022,
292 with three additional changes relative to its parent BA.5 (S:R346T, S:K444T, S:N460K). Similarly, the
293 recombinant XBB.1.1, circulating around the same time, had changes in several of the same
294 locations including S:R346T, S:L368I, S:N460K, S:F486S, S:R493Q and S:F490S. These two variants
295 were also resistant to neutralisation by panels of triple vaccinated volunteers in other studies as well
296 as in those with breakthrough infections with BA.1 and BA.2 [42, 43].

297 In the UK, as boosters containing bivalent antigens were deployed in the Autumn of 2022, we
298 continued our assessment of emerging variants with samples from individuals who had received a
299 BA.1/ancestral booster. The majority also had at least one breakthrough infection between February
300 2021 and December 2022 (Alpha to XBB.1.5). Results from this panel showed that neutralisation
301 titres for the two variants which were no longer neutralised by the three-dose panel (BQ.1.22 and
302 XBB.1.1) were effectively neutralised by this four-dose panel. Indeed, all the subsequent
303 recombinants and Omicron sub-lineages tested here showed similar neutralisation titres for all
304 variants between CH.1.1 to BA.2.86. This includes the two BA.2.86 isolates tested here, with and
305 without the presence of an amino acid change in the FCS (S:R682W), with no significant difference
306 seen for sera tested against the two viruses. These data are in alignment with others who have
307 demonstrated that changes in the FCS are not important in relation to virus neutralisation *in vitro*
308 but alter how the virus behaves *in vivo* [19-22]. Following the emergence of the BA.2.86 sub-lineage,
309 JN.1 (August 2023) and its subsequent declaration by the WHO as a VOI (19th December 2023), we
310 also isolated and investigated this variant [5]. JN.1 has a further amino acid change in the RBD in

311 addition to BA.2.86 (S:L455S) which has generated concern due to changes at this position in other
312 variants being associated with increased escape from humoral immunity [44].

313 All variants tested displayed increased resistance to neutralisation to this four-dose panel relative to
314 both ancestral and BA.4, with similar GM titres for all except JN.1 (CH.1.1, BQ.1.22, XBB.1.1, XBB.1.5,
315 XBB.1.16, XBB.2.3, EG.5.1.1, BA.2.86). This aligns with results presented by other groups using both
316 pseudovirus (PSV) and authentic virus assays against panels of vaccinated (three- and four-dose)
317 with additional break-through infection in a globally diverse population [45-52]. It is also of interest
318 that the GM titres, up to and including BA.2.86, are comparable despite the genetic diversity in the
319 variants tested against our four-dose panels. This is likely due to the range of variants to which these
320 individuals have acquired natural immunity via break-through infections. The fold-reduction of our
321 neutralisation titres against JN.1 relative to BA.2.86 are comparable to two studies using PSV assays
322 which demonstrated an approximate two-fold reduction [53, 54]. Two other studies, however,
323 demonstrated similar titres against both BA.2.86 and JN.1 [55, 56]. The serum samples used in these
324 studies were collected more recently than our own panel which could explain the differences seen
325 with our own results. A common observation from all of the published data is that sera from those
326 with a breakthrough infection since the emergence of late XBB variants such as XBB.1.5 or EG.5.1
327 have higher titres and broader cross-protection between variants. Another study generated
328 neutralisation data for the JN.1 variant used sera from XBB.1.5 vaccinated individuals. In that study,
329 the neutralisation titres were consistently higher against all variants, including JN.1, post
330 vaccination. BA.2.86 was not investigated in this study, however the fold-reductions for JN.1 relative
331 to XBB.1.5 (2.9 to 4.3-fold) were comparable to those estimated by our own study for these variants
332 (4.2-fold). We note however that, due to vaccination campaigns targeting at-risk subgroups within
333 the population, the sera or plasma from individuals in our panel of boosted vaccinees are part of a
334 limited subset of the population considered to be at risk. Whilst this is informative in terms of the
335 effects of vaccines on immunity it may be less representative of levels of vaccine-induced immunity
336 in the general population.

337 Antigenic mapping of the human data shows co-localisation of the pre-Omicron variants in the
338 centre of the map with a larger antigenic spread following the emergence of Omicron and
339 recombinants. This is comparable to maps presented by others using human data, though direct
340 comparisons are challenging given the diversity in vaccination, circulating variant exposure and
341 breakthrough infections in different panels of human sera used between studies [24, 57-60]. For
342 example, many will have had different vaccination schedules/ formulations and exposure to
343 unidentified viral variants in addition to human genetic diversity leading to a range of humoral
344 immune responses. However, while distances between variants in different maps may vary, the
345 general pattern is the same with pre-Omicron variants localised to the centre and clusters of related
346 variants moving out from the centre in a chronological manner. As others have shown, the XBB
347 family of variants cluster further away from ancestral than BA.4/5 and late Omicron variants such as
348 BQ.1.22, CH.1.1 and BA.2.86 are more distant again [52, 61]. Another study which mapped JN.1
349 antigenically also showed this variant as distinct from other variants, but it did not have data from
350 other late Omicron variants to enable comparison of how these may group together [62].

351 One limitation of ours and others human antigenic maps is the clustering of sera in one location on
352 the map, corresponding to the ancestral spike that drove the pandemic and was used as the basis of
353 the first-generation vaccines. This effect is less prominent when using the neutralisation titres from
354 sera taken from hamsters 27- or 28-days post-infection with a single, known SARS-CoV-2 variant at a
355 standard infectious dose. Antigenic mapping of these data highlighted two antigenically distinct
356 viruses: BQ.1.22 and XBB.1.1. Although the most contemporary variant to date, BA.2.86, is one of
357 the furthest antigenically from ancestral, it clustered closely with XBB.1.5. This suggests that
358 antibodies raised against the XBB.1.5 spike antigen have good cross-reactivity against BA.2.86, thus
359 supporting the transition to XBB.1.5 based vaccines. Others have also shown XBB.1.1, BQ.1.1 and
360 BA.2.86 to be distinct in antigenic maps generated with hamster or mouse data [52, 61]. Using single
361 exposure sera from hamsters has the added benefits of being generated by a known priming
362 antigen, given at the same dose with the duration since infection being known and fixed. These are

363 therefore more predictive of antigenic relationships when mapped. Our hamster data also indicate
364 that a BA.5 spike alone does not generate a detectable neutralising antibody response to one of the
365 most recent variants, BA.2.86. Taken together, these data suggested a turning point in the virus'
366 evolution and signalled to vaccine developers that an updated vaccine was required. On 18 May
367 2023 the WHO Technical Advisory Group on COVID-19 Vaccine Composition (TAG-CO-VAC) published
368 their recommendations to develop vaccines to target contemporary XBB-descendent lineages [63].

369 Numbers of sequenced SARS-CoV-2 genomes are decreasing due to reduced global surveillance
370 activity since the end of the pandemic. As a result, identifying variants of concern in a timely manner
371 is increasingly challenging. This was highlighted by the apparent sudden emergence of BA.2.86 in
372 August 2023 despite some models retrospectively predicting it had been circulating since May 2023
373 [48, 64]. Continued monitoring of emerging variants and their assessment in programmes such as
374 Agility is essential to build on existing knowledge of immune evasion of contemporary and newly
375 emerging variants and to better advise policymakers and vaccine manufacturers on future strategies.

376 **Methods**

377 Human vaccinee sera and antibody standards

378 SARS-CoV-2 variants were tested against two panels of vaccinee samples collected from staff
379 volunteers. The first panel, consisting of sera from individuals who had received three doses of an
380 ancestral spike-based COVID-19 vaccine, was collected as part of the ESCAPE study as previously
381 described [12, 65]. The second panel was assembled from staff members at MHRA (n=8 plasma
382 samples) and UKHSA (n=14 sera samples) who had received a fourth vaccination consisting of
383 bivalent (BA.1/ancestral) vaccine. Samples were collected at a median of 78 days after the fourth
384 vaccination. When tested for the presence of anti-N antibodies, 19 of the 22 individuals had
385 evidence of convalescence for naturally acquired SARS-CoV-2 infection. Dates of previous infections
386 were provided by 14 individuals which identified an infection range of February 2021 to December
387 2022. Two reference materials were included in this study: a working reagent for anti-SARS-CoV-2

388 immunoglobulin (NIBSC 21/234), which is a pool of several pre-Alpha convalescent plasma, and the
389 International Standard for antibodies to SARS-CoV-2 VOC (NIBSC 21/338), which is a pool of 265
390 individuals who are both vaccinated and convalescent following Alpha, Beta or Delta infection [66,
391 67].

392 Virus bank preparation and quality control checks

393 Unless otherwise stated in Table 1, viruses were isolated from sequence-confirmed clinical swabs at
394 UKHSA. SARS-CoV-2 variants were isolated and propagated on Vero/hSLAM cells (ECACC 04091501)
395 before being subjected to quality control checks as previously described [12]. Briefly, titrations were
396 performed using a focus-forming assay with immunostaining for nucleocapsid to visualise foci [68].
397 Sighting for each variant into the Focus Reduction Neutralisation Test (FRNT) to calculate dilution at
398 which a median of 130 foci could be counted in non-neutralised control wells was performed. Whole
399 genome sequencing (SISPA-Illumina) was performed on final virus assay banks, as described
400 previously, to confirm presence of FCS S1/S2 boundary, check for mixed bases as well as confirm
401 variant identity [12, 69-71]. A 12-nucleotide insertion (after position 21608) and nine-nucleotide
402 deletion (21633-21641) in BA.2.86 results in short illumina reads in this region which map poorly to
403 the reference sequence NC_045512.2. Therefore, BA.2.86, illumina sequence was mapped to Oxford
404 Nanopore Technologies (ONT) consensus sequence in place of NC_045512.2. Sequence data of the
405 virus banks used in the neutralisation tests in this study are available in Supplementary Data File S1.

406 FRNT and statistics

407 Median neutralising antibody titres (ND_{50}) were measured with FRNT and calculated with a Probit
408 regression analysis using R v4.1.2 (R Core Team, Vienna, Austria) as described previously [11, 12, 68].
409 Log_{10}-transformed ND_{50} titres were analysed using a mixed-effects linear model in R, as described
410 previously [12, 72].

411 Antigenic cartography

412 Antigenic maps were generated using the Racmacs (https://acorg.github.io/Racmacs/) package in R
413 as described previously [24, 73]. The number of dimensions was set to 2, number of optimisations to
414 500 and minimum column basis to none. Neutralisation titres from human and hamster sera were
415 used to generate two separate maps.

416 Hamster sera

417 All *in vivo* experimental work was conducted under the authority of a UK Home Office approved
418 project licence that has been subject to local ethical review at either UK Health Security Agency
419 Porton Down or Medicines and Healthcare products Regulatory Agency, South Mimms by their
420 respective Animal Welfare and Ethical Review Body (AWERB) as required by the *Home Office*
421 *Animals (Scientific Procedures) Act 1986*.

422 Sera collected at day 27 post-infection from hamsters exposed to ancestral virus (n=6) and BA.1
423 (n=5) or day 28 post-infection with BA.4 (n=6) and BA.5.2.1 (n=6). These hamster sera were
424 generated as previously described [27, 28]. Sera was collected from hamsters infected with XBB1.16
425 and XBB.2.3 (n=6 per variant) with a target dose of $1x10^4$ FFU/200 µL via intranasal instillation
426 (method previously described [27, 28]). Blood samples were collected during necropsy at 28 days
427 post infection.

428 Sera from XBB.1.5 convalescent hamsters were collected as follows. Four hamsters (approximately
429 10 weeks old) were administered $1x10^5$ FFU/50µL intranasally of XBB.1.5. After infection, oral swabs
430 were taken to confirm infection by lateral flow and RT-qPCR. Hamsters were terminated at 28 days
431 post-infection and clotted whole blood was centrifuged (1,000RPM, 5 mins) to obtain serum.

432

433 **Acknowledgements**

434 The authors gratefully acknowledge the support from the Porton Sequencing Laboratory and the
435 Biological Services Porton at the UK Health Security Agency, Porton Down, United Kingdom. The

authors thank our staff volunteers for providing serum and plasma samples so that we can assemble our testing panels. We also acknowledge Samuel Wilks and Derek Smith for their help and advice with using the Racmacs package. The authors are grateful to Professor Isabella Eckerle and Dr Meriem Bekliz for sharing sequence data for their Zeta variant and useful discussions.

Ethics

The ESCAPE study was conducted in accordance with the Declaration of Helsinki and the Governance Arrangements for Research Ethics Committees (GAfREC). It was approved by the PHE Research Ethics and Governance Group (R&D REGG Ref NR0190, March 2020). Informed consent was obtained from all subjects involved. Donations from MHRA staff members were collected with written informed consent from donors, study was approved by the MHRA local ethics committee (HuMAC ref: 20/05/SK).

References

1. Organization WH. WHO Coronavirus (COVID-19) Dashboard 2023 [cited 2023 27th September]. Available from: https://covid19.who.int/.
2. Organization WH. Statement on the fifteenth meeting of the IHR (2005) Emergency Committee on the COVID-19 pandemic 2023 [cited 2023 27th September]. Available from: https://www.who.int/news/item/05-05-2023-statement-on-the-fifteenth-meeting-of-the-international-health-regulations-(2005)-emergency-committee-regarding-the-coronavirus-disease-(covid-19)-pandemic.
3. O'Toole Á, Scher E, Underwood A, Jackson B, Hill V, McCrone JT, et al. Assignment of epidemiological lineages in an emerging pandemic using the pangolin tool. Virus Evolution. 2021;7(2). doi: 10.1093/ve/veab064.
4. Rambaut A, Holmes EC, O'Toole Á, Hill V, Mccrone JT, Ruis C, et al. A dynamic nomenclature proposal for SARS-CoV-2 lineages to assist genomic epidemiology. Nature Microbiology. 2020;5(11):1403-7. doi: 10.1038/s41564-020-0770-5.
5. WHO. Tracking SARS-CoV-2 variants 2023 [cited 2023 27th September]. Available from: https://www.who.int/en/activities/tracking-SARS-CoV-2-variants/.
6. England N. Landmark moment as first NHS patient receives COVID-19 vaccination 2020 [cited 2023 10th October]. Available from: https://www.england.nhs.uk/2020/12/landmark-moment-as-first-nhs-patient-receives-covid-19-vaccination/#:~:text=Landmark%20moment%20as%20first%20NHS%20patient%20receives%20COVID%2D19%20vaccination,-8%20December%202020&text=The%20biggest%20vaccine%20campaign%20in,jab%20following%20its%20clinical%20approval.
7. Care DoHaS. Second COVID-19 vaccine authorised by medicines regulator 2020 [cited 2023 10th October]. Available from: https://www.gov.uk/government/news/second-covid-19-vaccine-authorised-by-medicines-regulator.

8. Agency MaHpR. Moderna vaccine becomes third COVID-19 vaccine approved by UK regulator 2021 [cited 2023 10th October]. Available from: https://www.gov.uk/government/news/moderna-vaccine-becomes-third-covid-19-vaccine-approved-by-uk-regulator.
9. Watson OJ, Barnsley G, Toor J, Hogan AB, Winskill P, Ghani AC. Global impact of the first year of COVID-19 vaccination: a mathematical modelling study. Lancet Infect Dis. 2022;22(9):1293-302. Epub 20220623. doi: 10.1016/S1473-3099(22)00320-6. PubMed PMID: 35753318; PubMed Central PMCID: PMCPMC9225255.
10. TGHN. The Global Health Network - Covax Epidemic Preparedness Innovations - Agility 2023 [cited 2023 1st October]. Available from: https://epi.tghn.org/covax-overview/enabling-sciences/agility_epi/.
11. Bewley KR, Coombes NS, Gagnon L, McInroy L, Baker N, Shaik I, et al. Quantification of SARS-CoV-2 neutralizing antibody by wild-type plaque reduction neutralization, microneutralization and pseudotyped virus neutralization assays. Nat Protoc. 2021;16(6):3114-40. Epub 2021/04/25. doi: 10.1038/s41596-021-00536-y. PubMed PMID: 33893470.
12. Coombes NS, Bewley KR, Le Duff Y, Hurley M, Smith LJ, Weldon TM, et al. Assessment of the Biological Impact of SARS-CoV-2 Genetic Variation Using an Authentic Virus Neutralisation Assay with Convalescent Plasma, Vaccinee Sera, and Standard Reagents. Viruses. 2023;15(3). Epub 20230225. doi: 10.3390/v15030633. PubMed PMID: 36992342; PubMed Central PMCID: PMCPMC10056478.
13. MHRA. First bivalent COVID-19 booster vaccine approved by UK medicines regulator 2022 [cited 2022 5th December]. Available from: https://www.gov.uk/government/news/first-bivalent-covid-19-booster-vaccine-approved-by-uk-medicines-regulator.
14. FDA. Coronavirus (COVID-19) Update: FDA Authorizes Moderna, Pfizer-BioNTech Bivalent COVID-19 Vaccines for Use as a Booster Dose 2022 [cited 2022 5th December]. Available from: https://www.fda.gov/news-events/press-announcements/coronavirus-covid-19-update-fda-authorizes-moderna-pfizer-biontech-bivalent-covid-19-vaccines-use.
15. Prevention CfDCa. COVID-19 Vaccination Coverage and Vaccine Confidence Among Adults 2023 [cited 2023 16th October]. Available from: https://www.cdc.gov/vaccines/imz-managers/coverage/covidvaxview/interactive/adults.html.
16. Agency MaHpR. MHRA approves Moderna's adapted COVID-19 vaccine (Spikevax) that targets Omicron XBB.1.5 2023 [cited 2023 10th October]. Available from: https://www.gov.uk/government/news/mhra-approves-modernas-adapted-covid-19-vaccine-spikevax-that-targets-omicron-xbb15.
17. Agency MaHpR. MHRA approves Pfizer/BioNTech's adapted COVID-19 vaccine (Comirnaty) that targets Omicron XBB.1.5 2023 [cited 2023 10th October]. Available from: https://www.gov.uk/government/news/mhra-approves-pfizerbiontechs-adapted-covid-19-vaccine-comirnaty-that-targets-omicron-xbb15.
18. FDA. FDA Takes Action on Updated mRNA COVID-19 Vaccines to Better Protect Against Currently Circulating Variants 2023 [cited 2023 10th October]. Available from: https://www.fda.gov/news-events/press-announcements/fda-takes-action-updated-mrna-covid-19-vaccines-better-protect-against-currently-circulating.
19. Chan YA, Zhan SH. The Emergence of the Spike Furin Cleavage Site in SARS-CoV-2. Mol Biol Evol. 2022;39(1). doi: 10.1093/molbev/msab327. PubMed PMID: 34788836; PubMed Central PMCID: PMCPMC8689951.
20. Valleriani F, Jurisic L, Di Pancrazio C, Irelli R, Ciarrocchi E, Martino M, et al. A Deletion Encompassing the Furin Cleavage Site in the Spike Encoding Gene Does Not Alter SARS-CoV-2 Replication in Lung Tissues of Mink and Neutralization by Convalescent Human Serum Samples. Pathogens. 2022;11(10). Epub 20221006. doi: 10.3390/pathogens11101152. PubMed PMID: 36297209; PubMed Central PMCID: PMCPMC9609486.

21. Klimstra WB, Tilston-Lunel NL, Nambulli S, Boslett J, McMillen CM, Gilliland T, et al. SARS-CoV-2 growth, furin-cleavage-site adaptation and neutralization using serum from acutely infected hospitalized COVID-19 patients. J Gen Virol. 2020;101(11):1156-69. Epub 20200821. doi: 10.1099/jgv.0.001481. PubMed PMID: 32821033; PubMed Central PMCID: PMCPMC7879561.
22. Peacock TP, Goldhill DH, Zhou J, Baillon L, Frise R, Swann OC, et al. The furin cleavage site in the SARS-CoV-2 spike protein is required for transmission in ferrets. Nature Microbiology. 2021;6(7):899-909. doi: 10.1038/s41564-021-00908-w.
23. Bekliz M, Adea K, Vetter P, Eberhardt CS, Hosszu-Fellous K, Vu D-L, et al. Neutralization of ancestral SARS-CoV-2 and variants Alpha, Beta, Gamma, Delta, Zeta and Omicron by mRNA vaccination and infection-derived immunity through homologous and heterologous variants. 2021.
24. Wilks SH, Muhlemann B, Shen X, Tureli S, LeGresley EB, Netzl A, et al. Mapping SARS-CoV-2 antigenic relationships and serological responses. bioRxiv. 2023. Epub 20230616. doi: 10.1101/2022.01.28.477987. PubMed PMID: 35860221; PubMed Central PMCID: PMCPMC9298128.
25. Smith DJ, Lapedes AS, de Jong JC, Bestebroer TM, Rimmelzwaan GF, Osterhaus ADME, et al. Mapping the Antigenic and Genetic Evolution of Influenza Virus. Science. 2004;305(5682):371-6. doi: doi:10.1126/science.1097211.
26. Fonville JM, Wilks SH, James SL, Fox A, Ventresca M, Aban M, et al. Antibody landscapes after influenza virus infection or vaccination. Science. 2014;346(6212):996-1000. doi: doi:10.1126/science.1256427.
27. Ryan KA, Bewley KR, Watson RJ, Burton C, Carnell O, Cavell BE, et al. Syrian hamster convalescence from prototype SARS-CoV-2 confers measurable protection against the attenuated disease caused by the Omicron variant. PLoS Pathog. 2023;19(4):e1011293. Epub 20230404. doi: 10.1371/journal.ppat.1011293. PubMed PMID: 37014911; PubMed Central PMCID: PMCPMC10104347.
28. Davies ER, Ryan KA, Bewley KR, Coombes NS, Salguero FJ, Carnell OT, et al. The Omicron Sub-Variant BA.4 Displays a Remarkable Lack of Clinical Signs in a Golden Syrian Hamster Model of SARS-CoV-2 Infection. Viruses. 2023;15(5). Epub 20230510. doi: 10.3390/v15051133. PubMed PMID: 37243219; PubMed Central PMCID: PMCPMC10224153.
29. Basile K, Agius JE, Fong W, McPhie K, Fennel M, Ko D, et al. Genomic evolution of SARS-CoV-2 variants of concern under in vitro neutralising selection pressure following two doses of the Pfizer-BioNTech BNT162b2 COVID-19 vaccine. bioRxiv. 2023:2023.09.24.558921. doi: 10.1101/2023.09.24.558921.
30. Sanderson T, Hisner R, Donovan-Banfield Ia, Hartman H, Løchen A, Peacock TP, et al. A molnupiravir-associated mutational signature in global SARS-CoV-2 genomes. Nature. 2023. doi: 10.1038/s41586-023-06649-6.
31. Markov PV, Ghafari M, Beer M, Lythgoe K, Simmonds P, Stilianakis NI, et al. The evolution of SARS-CoV-2. Nature Reviews Microbiology. 2023;21(6):361-79. doi: 10.1038/s41579-023-00878-2.
32. Bekliz M, Adea K, Vetter P, Eberhardt CS, Hosszu-Fellous K, Vu DL, et al. Neutralization capacity of antibodies elicited through homologous or heterologous infection or vaccination against SARS-CoV-2 VOCs. Nat Commun. 2022;13(1):3840. Epub 2022/07/06. doi: 10.1038/s41467-022-31556-1. PubMed PMID: 35787633; PubMed Central PMCID: PMCPMC9253337 Technical Advisory Group (TAG) on Emergency Use Listing of COVID-19 vaccines. All other authors declare no competing interests.
33. Brun J, Vasiljevic S, Gangadharan B, Hensen M, V. Chandran A, Hill ML, et al. Assessing Antigen Structural Integrity through Glycosylation Analysis of the SARS-CoV-2 Viral Spike. ACS Central Science. 2021;7(4):586-93. doi: 10.1021/acscentsci.1c00058.
34. Kwilas S, Liesman RM, Zhang L, Walsh E, Pickles RJ, Peeples ME. Respiratory Syncytial Virus Grown in Vero Cells Contains a Truncated Attachment Protein That Alters Its Infectivity and Dependence on Glycosaminoglycans. Journal of Virology. 2009;83(20):10710-8. doi: 10.1128/jvi.00986-09.

35. Routhu NK, Lehoux SD, Rouse EA, Bidokhti MRM, Giron LB, Anzurez A, et al. Glycosylation of Zika Virus is Important in Host–Virus Interaction and Pathogenic Potential. International Journal of Molecular Sciences. 2019;20(20):5206. doi: 10.3390/ijms20205206.
36. Letarov AV, Babenko VV, Kulikov EE. Free SARS-CoV-2 Spike Protein S1 Particles May Play a Role in the Pathogenesis of COVID-19 Infection. Biochemistry (Mosc). 2021;86(3):257-61. doi: 10.1134/S0006297921030032. PubMed PMID: 33838638; PubMed Central PMCID: PMCPMC7772528.
37. Girgis S, Xu Z, Oikonomopoulos S, Fedorova AD, Tchesnokov EP, Gordon CJ, et al. Evolution of naturally arising SARS-CoV-2 defective interfering particles. Commun Biol. 2022;5(1):1140. Epub 20221027. doi: 10.1038/s42003-022-04058-5. PubMed PMID: 36302891; PubMed Central PMCID: PMCPMC9610340.
38. Miller NL, Clark T, Raman R, Sasisekharan R. Insights on the mutational landscape of the SARS-CoV-2 Omicron variant receptor-binding domain. Cell Rep Med. 2022;3(2):100527. Epub 20220124. doi: 10.1016/j.xcrm.2022.100527. PubMed PMID: 35233548; PubMed Central PMCID: PMCPMC8784435.
39. Greaney AJ, Starr TN, Bloom JD. An antibody-escape estimator for mutations to the SARS-CoV-2 receptor-binding domain. Virus Evolution. 2022;8(1). doi: 10.1093/ve/veac021.
40. Planas D, Bruel T, Staropoli I, Guivel-Benhassine F, Porrot F, Maes P, et al. Resistance of Omicron subvariants BA.2.75.2, BA.4.6, and BQ.1.1 to neutralizing antibodies. Nat Commun. 2023;14(1):824. Epub 20230214. doi: 10.1038/s41467-023-36561-6. PubMed PMID: 36788246; PubMed Central PMCID: PMCPMC9926440.
41. Dijokaite-Guraliuc A, Das R, Nutalai R, Zhou D, Mentzer AJ, Liu C, et al. Antigenic characterization of SARS-CoV-2 Omicron subvariant BA.4.6. Cell Discov. 2022;8(1):127. Epub 20221129. doi: 10.1038/s41421-022-00493-0. PubMed PMID: 36443292; PubMed Central PMCID: PMCPMC9705283.
42. Wang X, Jiang S, Jiang S, Li X, Ai J, Lin K, et al. Neutralization of SARS-CoV-2 BQ.1.1, CH.1.1, and XBB.1.5 by breakthrough infection sera from previous and recent waves in China. Cell Discov. 2023;9(1):64. Epub 20230627. doi: 10.1038/s41421-023-00569-5. PubMed PMID: 37369648; PubMed Central PMCID: PMCPMC10300020.
43. Jiang XL, Zhu KL, Wang XJ, Wang GL, Li YK, He XJ, et al. Omicron BQ.1 and BQ.1.1 escape neutralisation by omicron subvariant breakthrough infection. Lancet Infect Dis. 2023;23(1):28-30. doi: 10.1016/S1473-3099(22)00805-2. PubMed PMID: 36543471; PubMed Central PMCID: PMCPMC9762743.
44. Kosugi Y, Plianchaisuk A, Putri O, Uriu K, Kaku Y, Alfredo A. Hinay J, et al. Virological characteristics of the SARS-CoV-2 Omicron HK.3 variant harboring the “FLip” substitution. bioRxiv. 2023:2023.11.14.566985. doi: 10.1101/2023.11.14.566985.
45. Wang X, Jiang S, Ma W, Li X, Wei K, Xie F, et al. Enhanced neutralization of SARS-CoV-2 XBB sub-lineages and BA.2.86 by a tetravalent COVID-19 vaccine booster. bioRxiv. 2023:2023.09.14.557682. doi: 10.1101/2023.09.14.557682.
46. Qu P, Xu K, Faraone JN, Goodarzi N, Zheng Y-M, Carlin C, et al. Immune Evasion, Infectivity, and Fusogenicity of SARS-CoV-2 Omicron BA.2.86 and FLip Variants. bioRxiv. 2023:2023.09.11.557206. doi: 10.1101/2023.09.11.557206.
47. Hu Y, Zou J, Kurhade C, Deng X, Chang HC, Kim DK, et al. Less neutralization evasion of SARS-CoV-2 BA.2.86 than XBB sublineages and CH.1.1. bioRxiv. 2023:2023.09.10.557047. doi: 10.1101/2023.09.10.557047.
48. Khan K, Lustig G, Reedoy K, Jule Z, Römer C, Karim F, et al. Evolution and neutralization escape of the SARS-CoV-2 BA.2.86 subvariant. medRxiv. 2023:2023.09.08.23295250. doi: 10.1101/2023.09.08.23295250.
49. Uriu K, Ito J, Kosugi Y, Tanaka YL, Mugita Y, Guo Z, et al. Transmissibility, infectivity, and immune resistance of the SARS-CoV-2 BA.2.86 variant. bioRxiv. 2023:2023.09.07.556636. doi: 10.1101/2023.09.07.556636.

50. Lasrado N, Collier A-rY, Hachmann NP, Miller J, Rowe M, Schonberg ED, et al. Neutralization Escape by SARS-CoV-2 Omicron Subvariant BA.2.86. bioRxiv. 2023:2023.09.04.556272. doi: 10.1101/2023.09.04.556272.
51. Sheward DJ, Yang Y, Westerberg M, Öling S, Muschiol S, Sato K, et al. Sensitivity of BA.2.86 to prevailing neutralising antibody responses. bioRxiv. 2023:2023.09.02.556033. doi: 10.1101/2023.09.02.556033.
52. Yang S, Yu Y, Jian F, Song W, Yisimayi A, Chen X, et al. Antigenicity and infectivity characterisation of SARS-CoV-2 BA.2.86. Lancet Infect Dis. 2023. Epub 20230919. doi: 10.1016/s1473-3099(23)00573-x. PubMed PMID: 37738994.
53. Kaku Y, Okumura K, Padilla-Blanco M, Kosugi Y, Uriu K, Hinay AA, Jr., et al. Virological characteristics of the SARS-CoV-2 JN.1 variant. Lancet Infect Dis. 2024. Epub 20240103. doi: 10.1016/S1473-3099(23)00813-7. PubMed PMID: 38184005.
54. Yang S, Yu Y, Xu Y, Jian F, Song W, Yisimayi A, et al. Fast evolution of SARS-CoV-2 BA.2.86 to JN.1 under heavy immune pressure. Lancet Infect Dis. 2023. Epub 20231215. doi: 10.1016/S1473-3099(23)00744-2. PubMed PMID: 38109919.
55. Jeworowski LM, Muhlemann B, Walper F, Schmidt ML, Jansen J, Krumbholz A, et al. Humoral immune escape by current SARS-CoV-2 variants BA.2.86 and JN.1, December 2023. Euro Surveill. 2024;29(2). doi: 10.2807/1560-7917.ES.2024.29.2.2300740. PubMed PMID: 38214083; PubMed Central PMCID: PMCPMC10785204.
56. Planas D, Staropoli I, Michel V, Lemoine F, Donati F, Prot M, et al. Distinct evolution of SARS-CoV-2 Omicron XBB and BA.2.86 lineages combining increased fitness and antibody evasion. bioRxiv. 2023. Epub 20231206. doi: 10.1101/2023.11.20.567873. PubMed PMID: 38045308; PubMed Central PMCID: PMCPMC10690205.
57. Wang W, Lusvarghi S, Subramanian R, Epsi NJ, Wang R, Goguet E, et al. Antigenic cartography of well-characterized human sera shows SARS-CoV-2 neutralization differences based on infection and vaccination history. Cell Host Microbe. 2022;30(12):1745-58 e7. Epub 20221021. doi: 10.1016/j.chom.2022.10.012. PubMed PMID: 36356586; PubMed Central PMCID: PMCPMC9584854.
58. Straten Kvd, Guerra D, Gils MJv, Bontjer I, Caniels TG, Willigen HDGv, et al. Mapping the antigenic diversification of SARS-CoV-2. medRxiv. 2022:2022.01.03.21268582. doi: 10.1101/2022.01.03.21268582.
59. van der Straten K, Guerra D, van Gils MJ, Bontjer I, Caniels TG, van Willigen HDG, et al. Antigenic cartography using sera from sequence-confirmed SARS-CoV-2 variants of concern infections reveals antigenic divergence of Omicron. Immunity. 2022;55(9):1725-31 e4. Epub 20220805. doi: 10.1016/j.immuni.2022.07.018. PubMed PMID: 35973428; PubMed Central PMCID: PMCPMC9353602.
60. Astakhova EA, Morozov AA, Byazrova MG, Sukhova MM, Mikhailov AA, Minnegalieva AR, et al. Antigenic Cartography Indicates That the Omicron BA.1 and BA.4/BA.5 Variants Remain Antigenically Distant to Ancestral SARS-CoV-2 after Sputnik V Vaccination Followed by Homologous (Sputnik V) or Heterologous (Comirnaty) Revaccination. International Journal of Molecular Sciences. 2023;24(13):10493. PubMed PMID: doi:10.3390/ijms241310493.
61. Mykytyn AZ, Rosu ME, Kok A, Rissmann M, van Amerongen G, Geurtsvankessel C, et al. Antigenic mapping of emerging SARS-CoV-2 omicron variants BM.1.1.1, BQ.1.1, and XBB.1. Lancet Microbe. 2023;4(5):e294-e5. Epub 20230116. doi: 10.1016/S2666-5247(22)00384-6. PubMed PMID: 36657480; PubMed Central PMCID: PMCPMC9842387.
62. Wang Q, Guo Y, Bowen A, Mellis IA, Valdez R, Gherasim C, et al. XBB.1.5 monovalent mRNA vaccine booster elicits robust neutralizing antibodies against emerging SARS-CoV-2 variants. bioRxiv. 2023:2023.11.26.568730. doi: 10.1101/2023.11.26.568730.
63. Organization WH. Statement on the antigen composition of COVID-19 vaccines 2023 [cited 2023 27th September]. Available from: https://www.who.int/news/item/18-05-2023-statement-on-the-antigen-composition-of-covid-19-vaccines.

675 64. Rothstein AP, Qiu X, Robison K, Collins S, Muir G, Lu B, et al. Bayesian phylogenetics on
676 globally emerging SARS-CoV-2 variant BA.2.86 suggest global distribution and rapid evolution.
677 bioRxiv. 2023:2023.09.08.556912. doi: 10.1101/2023.09.08.556912.
678 65. Harris RJ, Whitaker HJ, Andrews NJ, Aiano F, Amin-Chowdhury Z, Flood J, et al. Serological
679 surveillance of SARS-CoV-2: Six-month trends and antibody response in a cohort of public health
680 workers. J Infect. 2021;82(5):162-9. Epub 2021/03/27. doi: 10.1016/j.jinf.2021.03.015. PubMed
681 PMID: 33766553; PubMed Central PMCID: PMCPMC7982645.
682 66. NIBSC. Working Standard Working reagent for anti-SARS-CoV-2 immunoglobulin NIBSC code:
683 21/234 2022 [cited 2022 12th December]. Available from: https://www.nibsc.org/documents/ifu/21-
684 234.pdf.
685 67. NIBSC. WHO International Standard 1st International Standard for antibodies to SARS-CoV-2
686 variants of concern NIBSC code: 21/338 2022 [cited 2022 12th December]. Available from:
687 https://www.nibsc.org/documents/ifu/21-338.pdf.
688 68. Ryan KA, Watson RJ, Bewley KR, Burton C, Carnell O, Cavell BE, et al. Convalescence from
689 prototype SARS-CoV-2 protects Syrian hamsters from disease caused by the Omicron variant. 2021.
690 69. Lewandowski K, Xu Y, Pullan ST, Lumley SF, Foster D, Sanderson N, et al. Metagenomic
691 Nanopore Sequencing of Influenza Virus Direct from Clinical Respiratory Samples. J Clin Microbiol.
692 2019;58(1). Epub 2019/11/02. doi: 10.1128/JCM.00963-19. PubMed PMID: 31666364; PubMed
693 Central PMCID: PMCPMC6935926.
694 70. Li H. Aligning sequence reads, clone sequences and assemblycontigs with BWA-MEM.
695 arXiv:13033997v2 [q-bioGN]. 2013.
696 71. Danecek P, Bonfield JK, Liddle J, Marshall J, Ohan V, Pollard MO, et al. Twelve years of
697 SAMtools and BCFtools. Gigascience. 2021;10(2). doi: 10.1093/gigascience/giab008. PubMed PMID:
698 33590861; PubMed Central PMCID: PMCPMC7931819.
699 72. R. R Core Team: A language and environment for statistical computing. R Foundation for
700 Statistical Computing 2014 [cited 2023 24th February]. Available from: http://www.R-project.org/.
701 73. Wilks S. Racmacs: Antigenic Cartography Macros 2023 [cited 2023 1st October]. Available
702 from: https://acorg.github.io/Racmacs/, https://github.com/acorg/Racmacs/.

703

704 **Supporting information captions**

705 **Table S1** – Summary of geometric mean neutralisation titres from a focus-reduction assay (FRNT) for
706 a panel of 10 triple vaccinated human sera against SARS-CoV-2 variants and their fold-changes
707 relative to ancestral virus. **Table S2** – Summary of geometric mean neutralisation titres from a focus-
708 reduction assay (FRNT) for a panel of 22 human sera/plasma taken from those who had received
709 three ancestral based vaccines as well as a BA.1/ancestral bivalent booster against SARS-CoV-2
710 variants. Fold-changes relative to ancestral virus are shown. **Table S3** – summary of geometric mean
711 neutralisation titres from a focus-reductions assay (FRNT) for a panel of sera taken from Syrian
712 hamsters (n=6) at day 27 post a single challenge with ancestral SARS-CoV-2. **Table S4** – summary of
713 geometric mean neutralisation titres from a focus-reductions assay (FRNT) for a panel of sera taken

714 from Syrian hamsters (n=5) at day 28 post a single challenge with the BA.1 SARS-CoV-2 variant. **Table**
715 **S5** – summary of geometric mean neutralisation titres from a focus-reductions assay (FRNT) for a
716 panel of sera taken from Syrian hamsters (n=6) at day 28 post a single challenge with the BA.4 SARS-
717 CoV-2 variant. **Table S6** – summary of geometric mean neutralisation titres from a focus-reductions
718 assay (FRNT) for a panel of sera taken from Syrian hamsters (n=6) at day 28 post a single challenge
719 with the BA.5.2.1 SARS-CoV-2 variant. **Table S7** – summary of geometric mean neutralisation titres
720 from a focus-reductions assay (FRNT) for a panel of sera taken from Syrian hamsters (n=4) at day 28
721 post a single challenge with the XBB.1.5 SARS-CoV-2 variant. **Table S8** – summary of geometric mean
722 neutralisation titres from a focus-reductions assay (FRNT) for a panel of sera taken from Syrian
723 hamsters (n=6) at day 28 post a single challenge with the XBB.1.16 SARS-CoV-2 variant. **Table S9** –
724 summary of geometric mean neutralisation titres from a focus-reductions assay (FRNT) for a panel of
725 sera taken from Syrian hamsters (n=6) at day 28 post a single challenge with the XBB.2.3 SARS-CoV-2
726 variant. **Supplementary data file - S1.fasta** – Sequence data of the virus banks used in the
727 neutralisation tests in this study

728

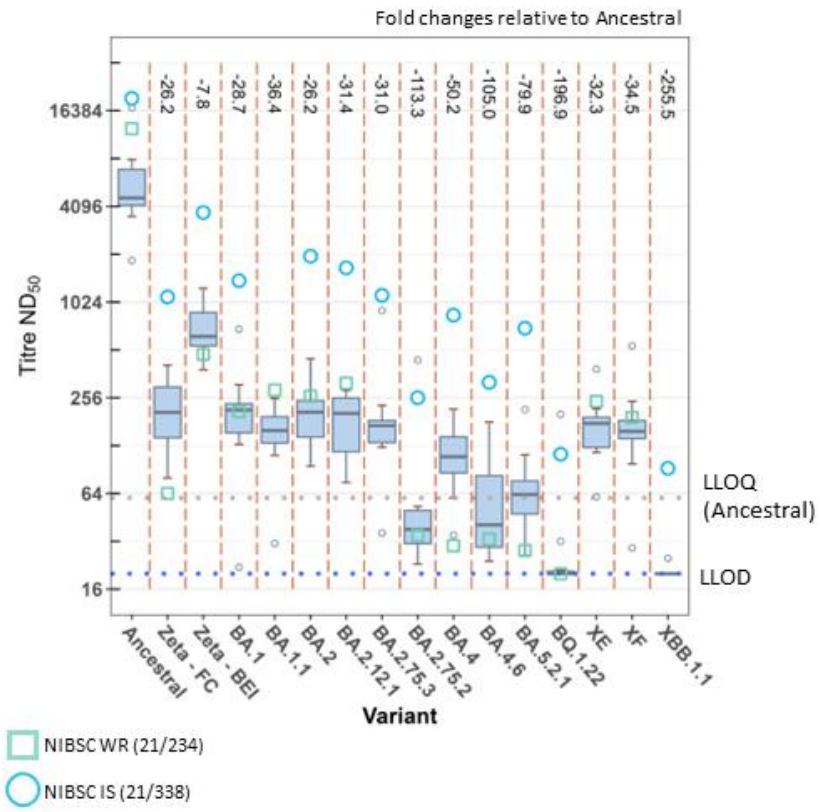

Figure 1. Neutralising antibody titres of a panel of triple vaccinated human participant sera determined by Focus Reduction Neutralisation Test (FRNT) against authentic SARS-CoV-2 Variants.

A panel of ten sera from triple vaccinated human volunteers were assessed by FRNT with 16 authentic SARS-CoV-2 variants. Data are presented as median and interquartile ranges of titre ND_{50}, titres of panel members falling outside of these ranges are plotted as open small circles. Fold-changes relative to ancestral virus were calculated by regression analysis using a mixed-effect model and are presented where the difference is statistically significant ($p<0.05$, two-way ANOVA with Tukey's *post hoc* test). The Lower Limit of Detection (LLOD) of 1/20 is indicated by the blue dotted line. The Lower Limit of Quantification (LLOQ) of 1/58 as determined for the ancestral assay, is indicated by the grey dotted line. Neutralisation titres of the standards; NIBSC WR 21/234 and 21/338, are presented as a green box and blue circle, respectively.

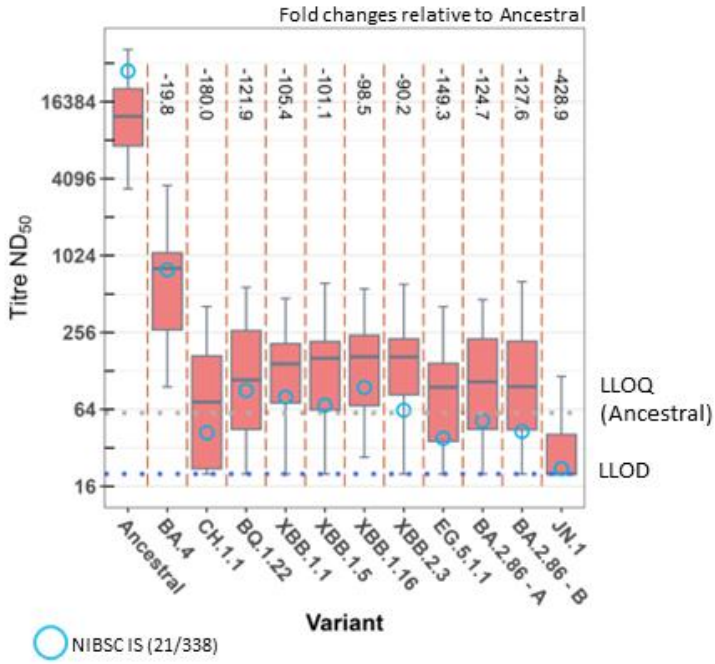

Figure 2. Neutralising antibody titres of a panel of sera/plasma from human volunteers who received three doses of an ancestral based vaccine as well as a BA.1 bivalent booster as determined by Focus Reduction Neutralisation Test (FRNT) against authentic SARS-CoV-2 Variants.

Sera/plasma from participants who received four doses of a vaccine were assessed by FRNT with 11 authentic SARS-CoV-2 variants. The panel consists of sera (n=14) and plasma (n=8) samples from human participants who received three doses of an ancestral based vaccine as well as a BA.1 bivalent booster. Of these, 19 out of 22 had at least one confirmed breakthrough infection with SARS-CoV-2. Data are presented as median and interquartile ranges of titre (ND_{50}). Fold-changes relative to ancestral virus were calculated by regression analysis using a linear mixed effect model and are presented where the difference is statistically significant ($p<0.05$, two-way ANOVA with Tukey's *post hoc* test). The Lower Limit of Detection (LLOD) of 1/20 is indicated by the blue dotted line. The Lower Limit of Quantification (LLOQ) of 1/58 as determined for the ancestral assay, is indicated by the grey dotted line. Neutralisation titres of the NIBSC WR 21/338 is presented as a blue circle.

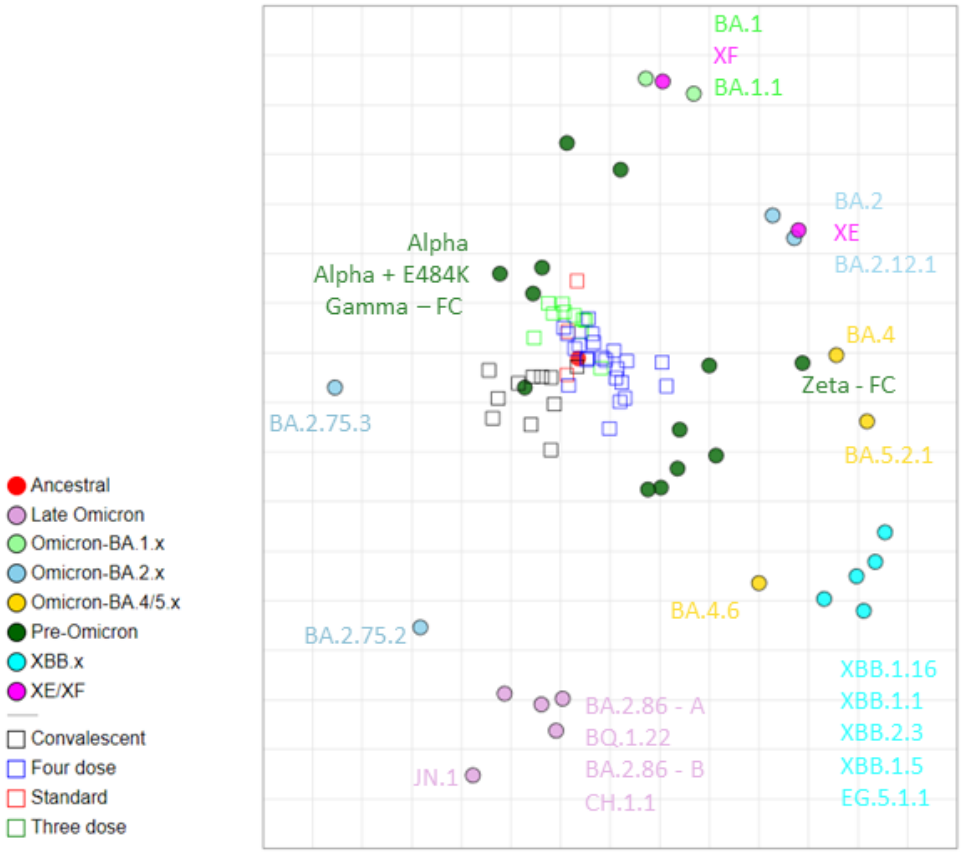

Figure 3. Antigenic map of SARS-CoV-2 variants assessed against human pre-Alpha convalescent, vaccinee sera or plasma and antibody standards

Median neutralisation titres (ND_{50}) for human sera/plasma were generated against 34 authentic SARS-CoV-2 variants and plotted as antigenic maps. Serum/Plasma are plotted as open-coloured boxes and virus variants (antigens) as filled circles. Convalescent plasma (n=11) collected early in the pandemic (pre-Alpha), sera (n=10) from triple-vaccinated individuals and sera/plasma (n=22) from those who had received a BA.1 bivalent booster are shown as black, green, and blue boxes, respectively. The standards, WHO IS 20/136, NIBSC WR 21/334 and IS 21/338 are also plotted as red boxes. Virus variants are shown as coloured circles.

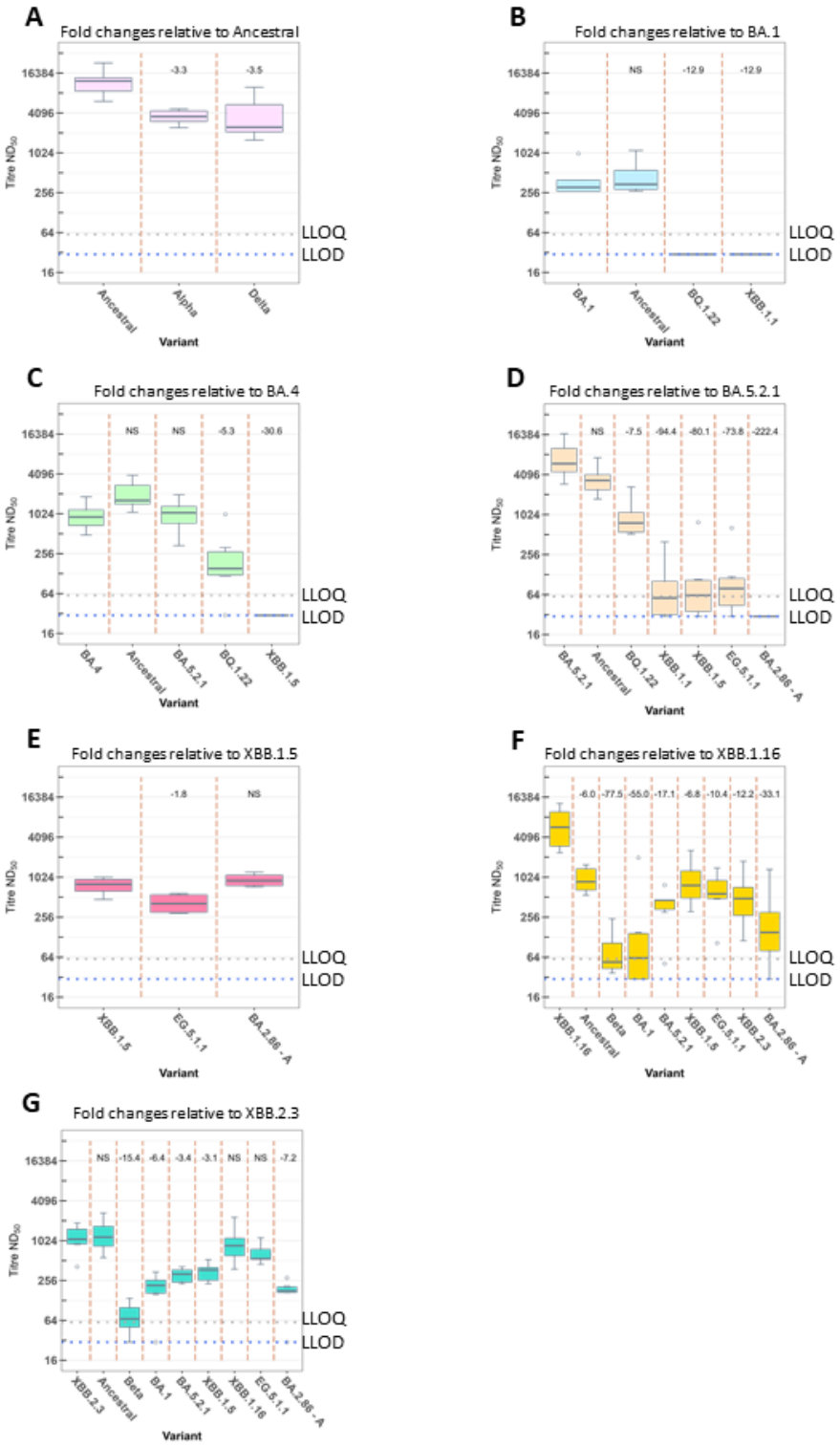
A
Fold changes relative to Ancestral
-3.3
-3.5
Ancestral
Alpha
Delta
B
Fold changes relative to BA.1
NS
-12.9
-12.9
BA.1
Ancestral
BQ.1.22
XBB.1.1
C
Fold changes relative to BA.4
NS
NS
-5.3
-30.6
BA.4
Ancestral
BA.5.2.1
BQ.1.22
XBB.1.5
D
Fold changes relative to BA.5.2.1
NS
-7.5
-94.4
-80.1
-73.8
-222.4
BA.5.2.1
Ancestral
BQ.1.22
XBB.1.1
XBB.1.5
EG.5.1.1
BA.2.86 - A
E
Fold changes relative to XBB.1.5
-1.8
NS
XBB.1.5
EG.5.1.1
BA.2.86 - A
F
Fold changes relative to XBB.1.16
-6.0
-77.5
-55.0
-17.1
-6.8
-10.4
-12.2
-33.1
XBB.1.16
Ancestral
Beta
BA.1
BA.5.2.1
XBB.1.5
EG.5.1.1
XBB.2.3
BA.2.86 - A
G
Fold changes relative to XBB.2.3
NS
-15.4
-6.4
-3.4
-3.1
NS
NS
-7.2
XBB.2.3
Ancestral
Beta
BA.1
BA.5.2.1
XBB.1.5
XBB.1.16
EG.5.1.1
BA.2.86 - A
Titre ND50
16384
4096
1024
256
64
16
LLOQ
LLOD
Variant

768

769 **Figure 4. Neutralising antibody titres of panels of convalescent sera from hamsters experimentally**
770 **infected with SARS-CoV-2 variants determined using an authentic virus Focus Reduction**
771 **Neutralisation Test (FRNT)**

772 Sera was collected from Golden Syrian hamsters at day 27 or day 28 post-infection with ancestral
773 (A), BA.1 (B), BA.4 (C), BA.5.2.1 (D), XBB.1.5 (E), XBB.1.16 (F) or XBB.2.3 (G) SARS-CoV-2 variants.
774 Median neutralisation titres (ND_{50}) were generated by FRNT using 14 authentic SARS-CoV-2 viruses.
775 Data are presented as median and interquartile ranges of titre (ND_{50}). Fold-changes relative to the
776 homologous virus were calculated by regression analysis using a mixed effect model and are
777 presented where the difference is statistically significant ($p<0.05$, two-way ANOVA with Tukey's *post*
778 *hoc* test). The Lower Limit of Detection (LLOD) of 1/30 is indicated by the blue dotted line. The Lower
779 Limit of Quantification (LLOQ) of 1/58 as determined for the ancestral assay, is indicated by the grey
780 dotted line. NS = not significant at the $p<0.05$ level.

781

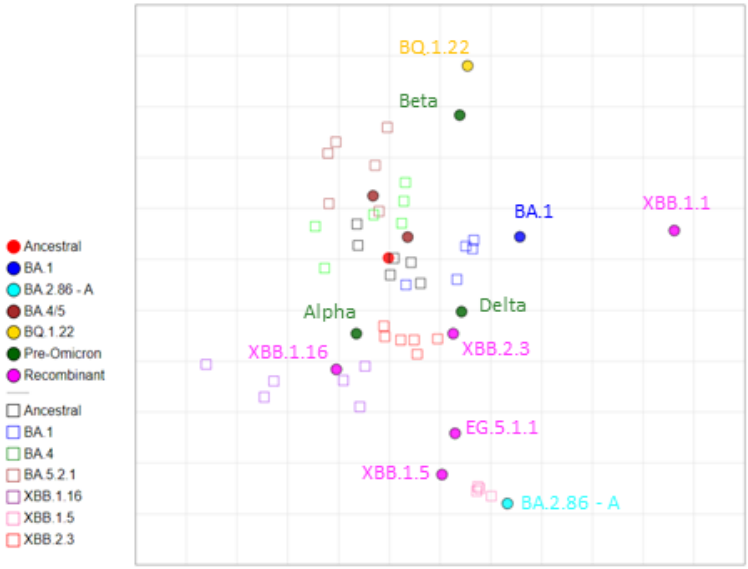

Figure 5. Antigenic map of SARS-CoV-2 variants assessed against convalescent sera collected from experimentally infected hamsters

Sera was collected from Golden Syrian hamsters at day 27 or day 28 post-infection with ancestral, BA.1, BA.4, BA.5.2.1, XBB.1.5, XBB.1.16 or XBB.2.3 SARS-CoV-2 variants. Median neutralisation titres (ND_{50}) were generated by Focus Reduction Neutralisation Test (FRNT) using 14 authentic SARS-CoV-2 viruses and plotted using antigenic cartography. Serum/Plasma are plotted as open-coloured boxes and virus variants (antigens) as filled circles.